SEARCH FOR NDE METHODS TO CHARACTERIZE THERMAL HISTORY AND MECHANICAL PROPERTIES OF Al-Li ALLOYS

D. J. Bracci, P. Garikepati, D. C. Jiles, and O. Buck

Center for NDE and Ames Laboratory, USDOE
Iowa State University
Ames, IA 50011

INTRODUCTION

Aluminum-lithium alloys have attracted the interest of the aerospace industry for some time now since the use of such alloys would reduce the weight of an airframe by roughly ten percent. The production of these alloys, however, requires precise thermal and/or thermomechanical treatments to insure required material properties, such as the yield strength and ductility. On-line monitoring of the state of the material thus seems to be desirable for quality control of these materials. This paper presents results of an investigation of fieldable NDE methods capable of providing information on the state of the material. Eddy current measurements were found to be particularly sensitive to Li in solid solution. Furthermore, it appears that hardness measurements are sensitive to the volume fractions, and probably the morphology, of the various precipitates formed. The results obtained so far (see also [1]) as well as by other authors on different aluminum alloys [2-4], this work will continue with additional results to be reported in future publications.

EXPERIMENTAL PROCEDURES

Materials used in this investigation were binary Al-2.2 wt% Li and Al 2090, the latter kindly provided by Alcoa [5], with a composition of about 2.7% Cu, 2.2% Li, 0.12% Zr, 0.08% Si, and 0.12% Fe (all in wt%). Heat treatments were as follows: Cooling rates after solid solution treatment at 430°C for the binary and 540°C for Al 2090 were, roughly, 130°C/sec for a fast quench in water (WQ) and about 100°C/min for the air cooled (AC) materials, as determined by a thermocouple attached to the specimens. Thereafter, aging temperatures between 150° and 200°C (in argon) with aging times between 0 and 33h were chosen. Transmission electron microscopy (TEM) studies are planned to investigate the volume fractions of the various metastable and stable phases, present in the two alloys. Flat specimens were used to determine the eddy current (EC) response at 5kHz, the DC resistivity, the microhardness (DPH), the elastic modulus (determined by the sound velocity at 10MHz) and the attenuation (determined by the amplitude decay of successive pulses at 10MHz). The mechanical properties were obtained using standard type tensile specimens. The 0.2% offset yield stress, σ_o, and the strain-

to-failure, ε_f, were determined by means of an Instron screw-driven deformation machine at a strain rate of about 1.6×10^{-4} sec^{-1}.

RESULTS

Examples of variation in hardness (DPH) and the reactive component of the eddy current response (ΔX) as a function of aging time and dependence are shown in Fig. 1 for the water quenched binary. Similar results have been obtained for both alloys, water quenched and air cooled. In the following, these results are summarized eliminating the time as a parameter. For example, the results shown in Fig. 1 have been replotted in Fig. 2, demonstrating that DPH is proportional to ΔX over the range of aging times and temperatures chosen. Note that the aging time increases from the lower left hand to the upper right hand corner. A similar result has been obtained for the air cooled binary, as shown in Fig. 2 although certain deviations from the proportionality can be noticed which are probably due to some nucleation of precipitates during air cool.

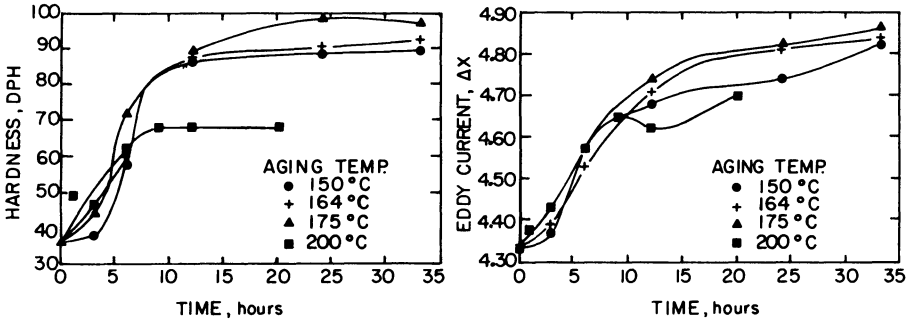

Fig. 1. Hardness (DPH) and reactive component of EC (ΔX) changes with aging time and temperature for a water quenched binary.

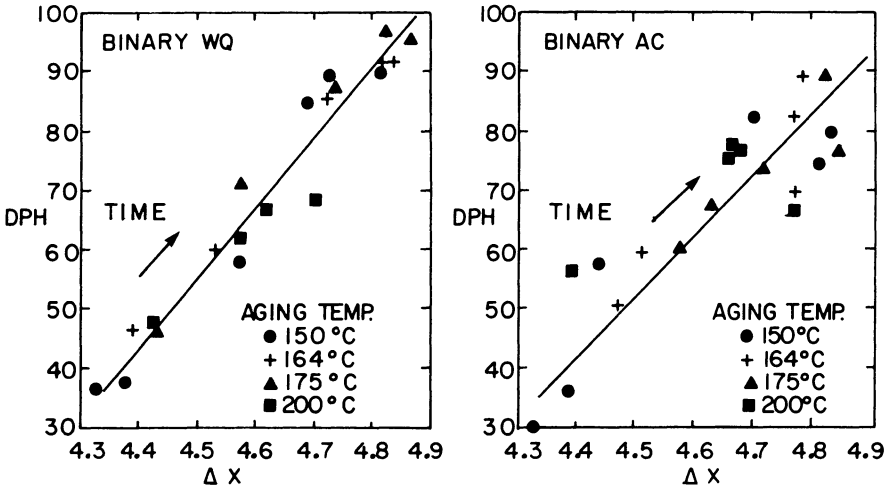

Fig. 2. DPH as a function of ΔX for the binary alloy.

Results obtained on water quenched Al 2090 are shown in Fig. 3. For the lower aging temperatures, DPH and ΔX are, again, proportional. However, there is a dramatic deviation from proportionality after aging at longer times at 200°C. At present, we believe that proportionality is maintained during δ' and T_1' precipitation. The strong deviations from proportionality may be caused by the formation of the T_2' phase [6]. TEM will be applied to clarify the situation. Figure 4 shows the observed correlations between the reactive component, ΔX, and the measured DC resistivity for the water quenched binary. As will be discussed later, the DC resistivity is strongly affected by lithium in solid solution. Therefore, the figure clearly demonstrates the capability of the eddy current measurements to determine lithium in solid solution. In contrast to the DPH and ΔX measurements, the elastic modulus and acoustic attenuation measurements, both performed at 10MHz, did not show any significant changes during aging.

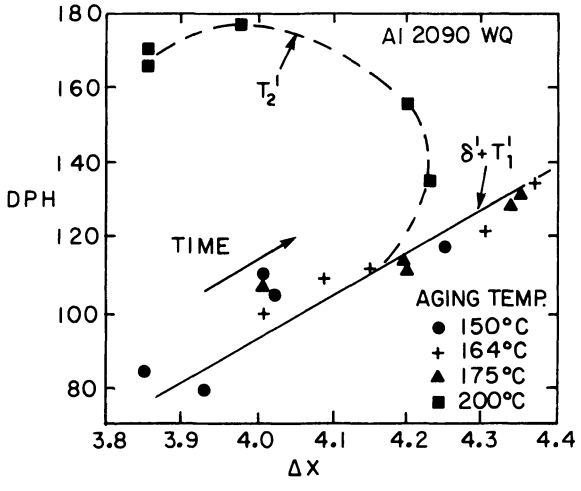

Fig. 3. DPH as a function of ΔX for Al 2090.

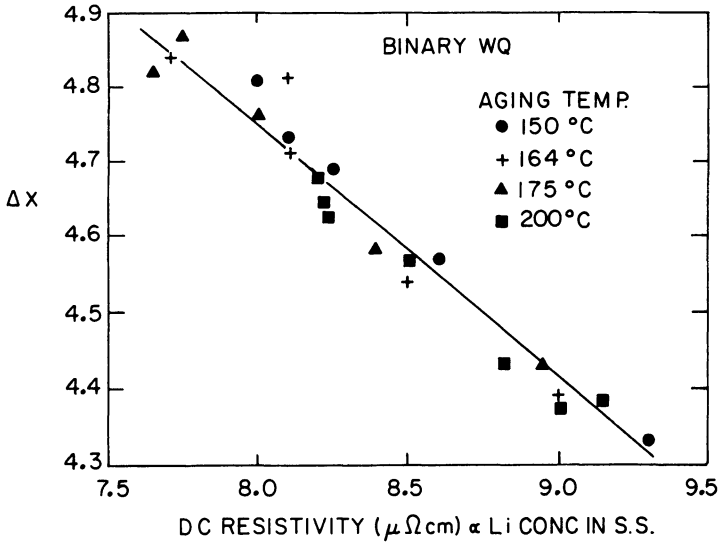

Fig. 4. ΔX versus DC resistivity and Li concentration in solid solution.

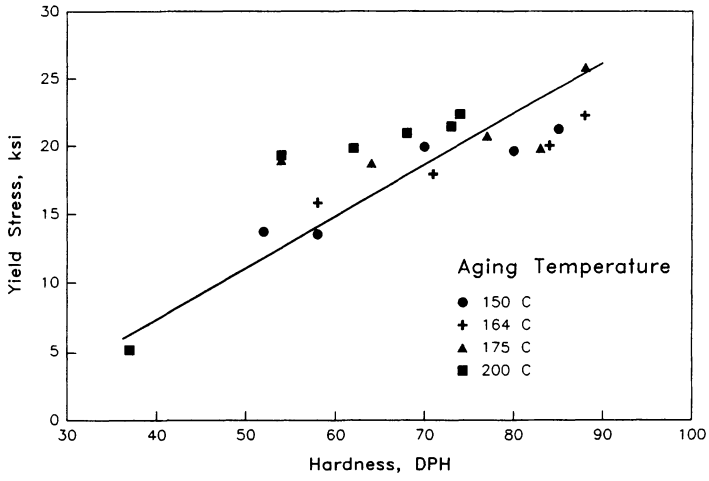

Fig. 5. Yield stress versus DPH for the water quenched binary.

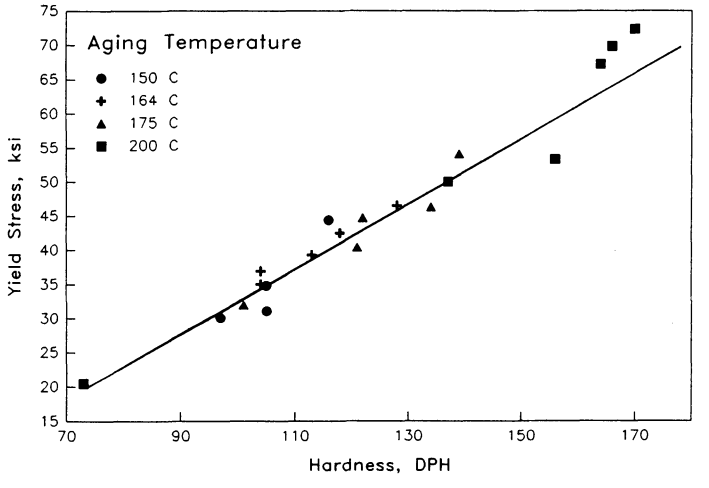

Fig. 6. Yield stress versus DPH for water quenched Al 2090.

The observed yield stress, σ_o, as a function of DPH for the water quenched binary is given in Fig. 5 (the air cooled binary yields a similar result) and for water quenched Al 2090 in Fig. 6. In both cases, σ_o increases continuously with hardness.

Strain to failure, ε_f, as a function of DPH is given for the water quenched binary in Fig. 7 and for the water quenched Al 2090 in Fig. 8. ε_f of the water quenched binary decreases continuously with increasing DPH, as expected. The changes in ε_f of the water quenched Al 2090 do not follow these expectations. It should be noted, however, that the relative changes in ε_f are small for this alloy, as may be seen comparing Fig. 8 with 7. We suspect at present that the uncertainty in determining ε_f may contribute, in part, to some of the unexpected trends.

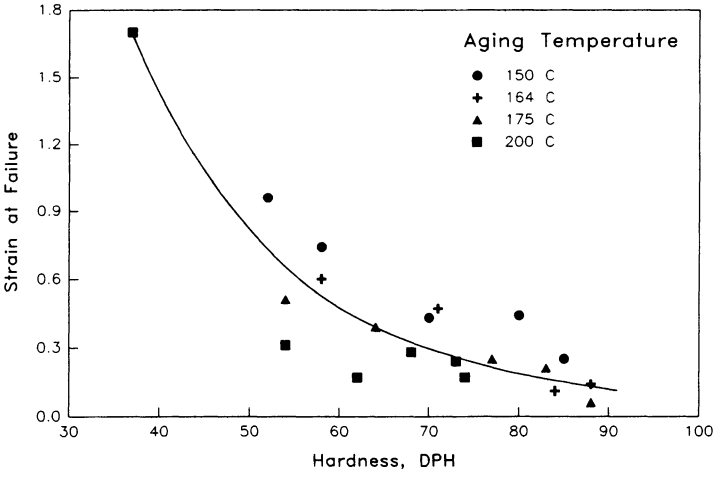

Fig. 7. Strain-to-failure versus DPH for the water quenched binary.

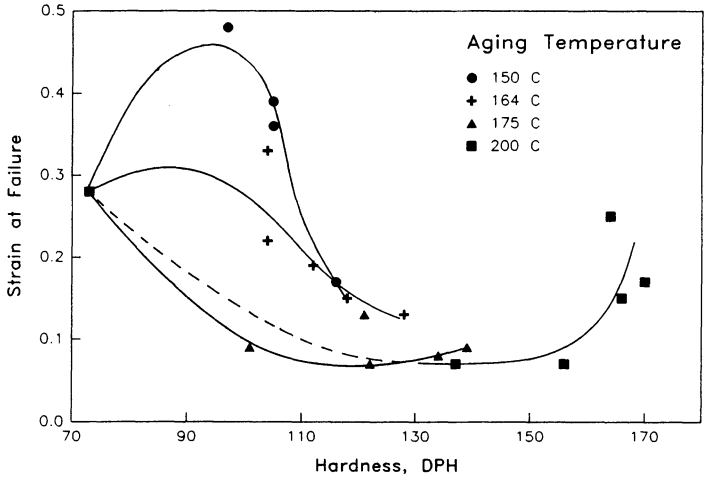

Fig. 8. Strain-to-failure versus DPH for water quenched Al 2090.

DISCUSSION AND CONCLUSIONS

A binary Al-2.2 wt% Li and a commercial Al 2090 alloy have been quenched from the solid solution phase at two different rates. Subsequent aging between 150 and 200°C with aging times ranging from 0 to 33h were chosen to obtain alloys of different microstructures and mechanical properties. Nondestructive measurements of the eddy current response (at 5kHz), the DC resistivity, the microhardness, as well as the elastic modulus and attenuation (both at 10MHz) have been performed on the different microstructures. It was found that the reactive component of EC and the DC resistivity change by roughly 5-10%. Hardness changes are about two-fold for Al 2090 and about three-fold for the binary alloy. The elastic modulus as well as the attenuation were found to be basically

independent of heat treatment. These latter results are different from those noted by Rosen et al. [7] for Al 2094. In their studies [7] the alloy was pre-aged, however, which leads to stable precipitate phases which was not the case in the present studies.

The yield stress of the alloys increases by about a factor of two and the strain-to-failure of the binary alloy decreases by about a factor of five. In general, the strain-to-failure of Al 2090 also decreases; however, we have not observed a systematic trend in these results as yet.

First correlations between the mechanical properties, σ_o and ε_f, and the various properties, characterized nondestructively, have been obtained. In general, σ_o increases and ε_f decreases with DPH (with certain exemptions, mentioned above). DPH and ΔX are proportional. The only exception to this rule, within the range of measurements performed so far, is probably due to T_2' phase formation [6]. This observation indicates the need for a transmission electron microscopy investigation to determine the volume fraction and morphology of the precipitates present in the alloys.

A preliminary data analysis of the reactive component of EC, ΔX, and the DC resistivity was performed, based on data partially shown in Fig. 4. The figure demonstrates that ΔX is linearly dependent on DC resistivity. In general, the DC resistivity is strongly determined by individual point defects or, in the present case, by Li in solid solution. As clusters form, the DC resistivity per atom drops off very rapidly [8]. ΔX is therefore determined by the Li in solid solution, rather than by the precipitates. Thus, the ΔX is due to the disappearance of Li from solid solution. Its emergence in the increase form of precipitates has little effect on ΔX. Therefore, one can assume that this is a "diffusion-limited" precipitation process [9] in which case the precipitates are homogeneously distributed throughout the lattice, as indicated in Fig. 9. The bulk concentration decreases with time as [9]

$$\bar{c} \propto c_o \exp[-(t/\tau)^n] \tag{1}$$

where $\bar{c}$ is the average concentration at time t, c_o the initial concentration, and τ is a "relaxation time", determined by the diffusion coefficient. Ham [9] found that for short times n=1.5 and for long times n=1.0. Converting the concentration $\bar{c}$ to ΔX values, Eq. (1) yields

$$\ln \frac{\Delta X_\infty - \Delta X}{\Delta X_\infty - \Delta X_o} \propto -(t/\tau)^n \tag{2}$$

where ΔX_∞ is the reactive component of EC when basically all Li has precipitated out, ΔX_o is the initial reactive component with all Li in solid solution and ΔX the reactive component at time t. Figure 10a shows such a plot for n=1.5, demonstrating the expected short time diffusion behavior. Figure 10b, on the other hand, shows a plot for n=1.0, demonstrating the expected long time diffusion behavior. As also can be seen from Fig. 10b, the slope at longer aging times is clearly temperature dependent. This temperature dependence is caused by the relaxation time τ in Eq. (1), given by

$$\tau = \tau_o \exp(E/kT) \tag{3}$$

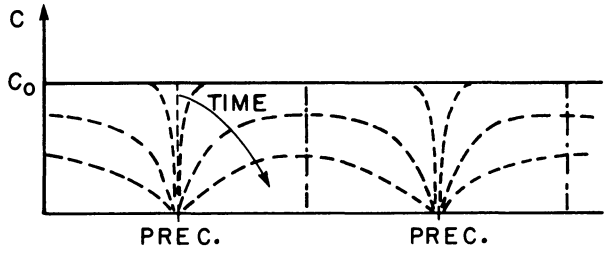

Fig. 9. Model for diffusion-limited precipitation.

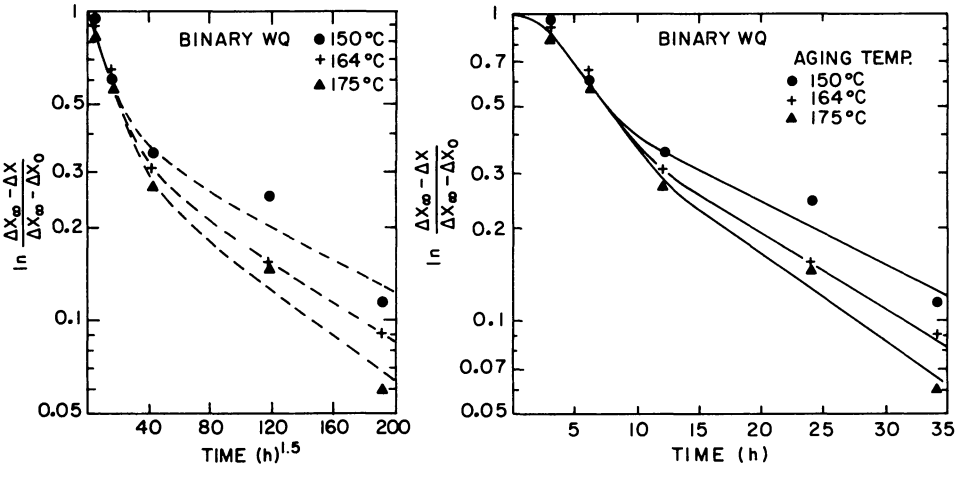

Fig. 10. Relative change of ΔX as a function of aging time and temperature for the water quenched binary; a) for n=1.5; b) for n=1.0.

where E is the activation energy of migration for Li in Al. Thus it appears as if the reactive component of EC provides basic information on the presence of Li in solid solution. Further evaluation is in progress, including modeling of DPH which is mainly caused by the precipitates themselves.

In conclusion, it appears that DC resistivity and/or the reactive component ΔX of the eddy current measurements, as well as the microhardness are prime indicators for the mechanical properties of Al-Li alloys, as noted before [3,4]. Both DC resistivity as well as ΔX provide information on Li in solid solutions. The contributions to the hardness are mainly due to precipitate formation. The individual phases will have to be determined by transmission electron microscopy so that estimates of their contributions to DPH can be obtained.

ACKNOWLEDGEMENT

The work was sponsored by the Center for NDE at Iowa State University and was performed at the Ames Laboratory. Ames Laboratory is operated for the U.S. Department of Energy by Iowa State University under Contract No. W-7405-ENG-82.

REFERENCES

1. D. J. Bracci, P. Garikepati, D. C. Jiles, and O. Buck, in Review of Progress in Quantitative NDE, 6B, D. O. Thompson and D. E. Chimenti, Eds., Plenum Press, NY, 1987, p. 1395.
2. W. D. Rummel, Materials Evaluation 24, 322 (1966).
3. L. J. Swartzendruber, W. J. Boettinger, L. K. Ives, S. R. Coriell, and R. Mehrabian, in "Nondestructive Evaluation: Microstructural Characterization and Reliability Strategies", O. Buck and S. M. Wolf, Eds., The Metallurgical Society of AIME, 1981, p. 253.
4. R. A. Chihoski, in "Nondestructive Methods for Material Property Determination", C. O. Ruud and R. E. Green, Eds., Plenum Press, NY, 1984, p. 81.
5. The authors appreciate several pieces of Al 2090, received from Alcoa.
6. R. J. Rioja and E. A. Ludwiczak, in "Aluminum-Lithium Alloys III", C. Baker, P. J. Gregson, S. J. Harris, and C. J. Peel, Eds., The Institute of Metals, London, 1986, p. 471.
7. M. Rosen, L. Ives, S. Ridder, F. Biancaniello, and R. Mehrabian, Mat. Science and Engr. 74, 1 (1985).
8. A. C. Damask and G. J. Dienes, "Point Defects in Metals", Gordon and Breach, NY, 1963.
9. F. S. Ham, J. Phys. Chem. Solids 6, 335 (1958).